Broadband terahertz lasing in aligned molecules

Andrew G. York[1,2]**, H. M. Milchberg**[1−4]

[1]*Institute for Research in Electronics and Applied Physics,* [2]*Department of Physics*
[3]*Institute for Physical Science and Technology,* [4]*ECE Department,*
University of Maryland, College Park, MD 20742, USA

Andrew.G.York+opex@gmail.com

Abstract: No broadband amplifying medium has been demonstrated yet for terahertz radiation. We present simulations showing that laser-aligned molecules can amplify broadband terahertz radiation, allowing high-energy amplification of few-cycle pulses at terahertz frequencies.

References and links

1. Y. Shen, T. Watanabe, D. A. Arena, C.-C. Kao, J. B. Murphy, T. Y. Tsang, X. J. Wang, and G. L. Carr "Nonlinear Cross-Phase Modulation with Intense Single-Cycle Terahertz Pulses," Phys. Rev. Lett. **99**, 043901 (2007).
2. C. H. Townes and A. L. Schawlow, *Microwave Spectroscopy* (McGraw-Hill, New York, 1955).
3. H. Harde and D. Grischkowsky,"Coherent transients excited by subpicosecond pulses of terahertz radiation," J. Opt. Soc. Am. B 8, 1642-1651 (1991).
4. Y. -H. Chen, S. Varma, A. York, and H. M. Milchberg, "Single-shot, space- and time-resolved measurement of rotational wavepacket revivals in H2, D2, N2, O2, and N2O," Opt. Express **15**, 11341-11357 (2007).
5. S. Ramakrishna and T. Seideman, "Dissipative dynamics of laser induced nonadiabatic molecular alignment," J. Chem. Phys. **124** 034101 (2006).
6. J. O. Hirschfelder and C. F. Curtiss, "Molecular Theory of Gases and Liquids" (John Wiley & Sons, Inc., New York, 1954).
7. C. H. Lin, J. P. Heritage, T. K. Gustafson, R. Y. Chiao, and J. P. McTague, "Birefringence arising from the reorientation of the polarizability anisotropy of molecules in collisionless gases," Phys. Rev. A **13** 813-829 (1976).
8. D. V. Kartashov, A. V. Kisrsanov, A. M. Kiselev, A. N. Stepanov, N. N. Bochkarev, Yu. N. Ponomarev, and B. A. Tikhomirov, "Nonlinear absorption of intense femtosecond laser radiation in air," Opt. Express **14** 7552-7558 (2006).
9. A. G. Smith, W. Gordy, J. W. Simmons, and W. V. Smith "Microwave Spectroscopy in the Region of Three to Five Millimeters," Phys. Rev. **75** 260-263 (1949).
10. V. Kumarappan, C. Z. Bisgaard, S. S. Viftrup, L. Holmegaard, and H. Stapelfeldt, "Role of rotational temperature in adiabatic molecular alignment," J. Chem. Phys **125**, 194309-1 -194309-7 (2006).
11. For example, the Coherent SIFIR-50
12. A. T. Rosenberger, H. K. Chung, and T. A. De Temple "Sub-T_2 Optical Pulse Generation: Application to Optically Pumped Far-Infrared Lasers," IEE J. Quantum Electron., **QE-20** 523-532 (1984).

1. Introduction

Broadband chirped-pulse amplification (CPA) in Ti:sapphire revolutionized nonlinear optics in the 90's, bringing intense optical pulses out of large government facilities and into the hands of graduate students in small university labs. Intense terahertz pulses ($\gg 10\mu$J, < 5 cycles), however, are still only produced at large accelerator facilities like BNL [1]. CPA is theoretically possible for terahertz frequencies, but no broadband lasing medium like Ti:sapphire has been demonstrated for terahertz. Dipolar molecular gases such as hydrogen cyanide (HCN)
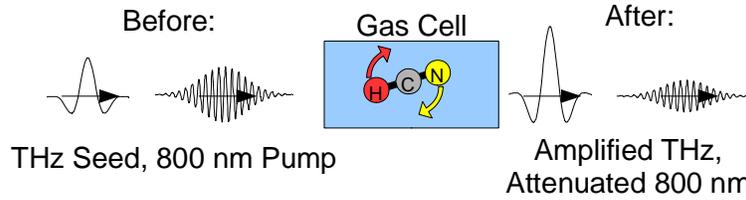
Fig. 1. Proposed broadband terahertz amplification

or nitrous oxide (N$_2$O), 'aligned' or rotationally excited by intense optical pulses, are a novel and promising medium for amplification of broadband few-cycle terahertz pulses. We present calculations that show rotationally excited molecules can amplify a few-cycle seed pulse of terahertz radiation, as shown in Fig. 1: a short, intense optical pulse (or sequence of pulses) aligns a dipolar gas (such as HCN), driving the molecules into a broad superposition of excited rotational states. A broadband seed terahertz pulse following the optical pulses can then be amplified on many pure rotational transitions simultaneously.

Since HCN or N$_2$O have a dipole moment, they can absorb and emit radiation through rotational transitions. The rotational spectrum of a gas of linear molecules is a series of regularly spaced lines in the low-terahertz frequency range [2]. Absorption and emission depend on the state of the gas; in thermal equilibrium, the rotational spectrum is purely absorbing [3]. Following intense, femtosecond optical pumping, however, molecular gas is driven into an 'aligned' excited rotational state [4]; the terahertz spectrum of this excited state is strongly modified. If the gas is sufficiently excited, its rotational spectrum contains a set of regularly spaced amplification lines. The duration of the 'aligned' excited state is determined by collisions. The pressure-dependent alignment lifetime of small linear molecules is tens or hundreds of picoseconds at or below atmospheric pressure (68.5 ps for N$_2$O at 1 atm [4]), and increases linearly with decreasing pressure. A few-cycle terahertz seed pulse could follow a few picoseconds behind an optical pump pulse train and be strongly amplified by many of these lines simultaneously.

2. Nonperturbative calculation of laser-molecule and THz-molecule interaction

We perform full-scale nonperturbative numerical simulations of the rotational quantum state of a gas of HCN molecules illuminated by femtosecond optical and terahertz pulses. Starting from the rigid-rotor density matrix model used in [4, 5], we represent an HCN molecule's rotational state $\Psi(\theta, \phi)$ as a superposition of spherical harmonics $|j, m\rangle$, where j is the rotational angular momentum quantum number and m is the quantum number corresponding to component of angular momentum along the laser or terahertz pulses' electric field. We define a density matrix $\boldsymbol{\rho} = \sum_{j,k,m} \rho_{j,k}^m |j, m\rangle\langle k, m|$. $\boldsymbol{\rho}$ describes the quantum state of an ensemble of identical, noninteracting HCN molecules subjected to the same linearly polarized electromagnetic field, such as a volume of gas much smaller than one cubic optical wavelength.

Similarly to [4, 5], $\boldsymbol{\rho}$ time-evolves according to:

$$
\begin{aligned}
\frac{d}{dt}\rho_{j,k}^m(t) = {} & -i\omega_{j,k}\rho_{j,k}^m(t) - (d\rho_{j,k}^m/dt)_{\text{diss}} + \\
& \frac{-i\Delta\alpha}{4\hbar}E_{\text{optical}}^2(t)\sum_q [O_{j,q}^m \rho_{q,k}^m(t) - O_{q,k}^m \rho_{j,q}^m(t)] + \\
& \frac{-i\mu}{\hbar}E_{\text{terahertz}}(t)\sum_q [T_{j,q}^m \rho_{q,k}^m(t) - T_{q,k}^m \rho_{j,q}^m(t)]
\end{aligned}
\tag{1}
$$

Here $\omega_{j,k} = \omega_j - \omega_k$, $\omega_j = 2\pi f_0 j(j+1)$, $\Delta\alpha$ is the difference in the molecule's parallel and
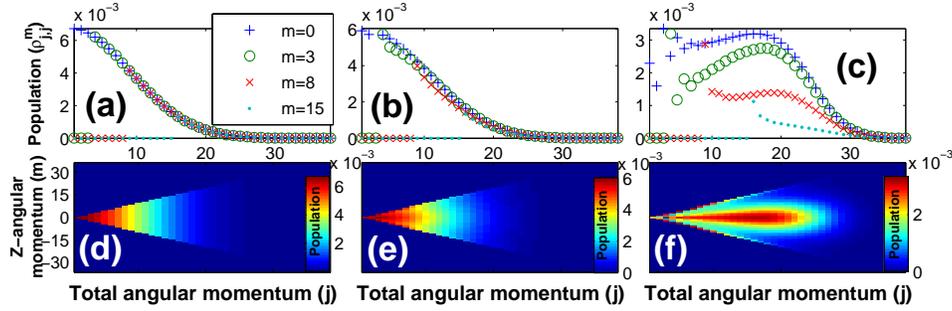
Fig. 2. Rotational state populations ρ_{jj}^m vs. j of HCN gas for selected m-values **(a)** before illumination (thermal population), (b) after illumination by a 15TW/cm^2, 100fs, 800nm optical alignment pulse, and (c) after a train of four such pulses separated by 11.49ps (the revival time of HCN). Below are intensity plots of ρ_{jj}^m vs. j and m for (d) thermal, (e) one-pulse, and (f) four-pulse illumination.

perpendicular polarizability and μ is its permanent dipole moment; For HCN $f_0 = 43.5$GHz (corresponding to rotational constant $B = 1.452$cm^{-1}), $\Delta\alpha = 2\text{Å}^3$, and $\mu = 3$ Debye [2, 6]. $E_{\text{optical}}^2(t)$ is the squared envelope of the nonresonant optical electric field, and $E_{\text{terahertz}}(t)$ is the full electric field (not the envelope) of the terahertz seed pulse [3, 7]. $O_{j,k}^m$ and $T_{j,k}^m$ describe how optical (O) and terahertz (T) radiation couple different elements of the density matrix. $O_{j,k}^m = \langle j,m|\cos^2(\theta)|k,m\rangle$, which is zero unless $j = k$ or $j = k \pm 2$, so optical radiation drives coherence only between states with the same parity [4]. Sufficiently intense optical radiation can be nonlinearly absorbed (or emitted) by $j \to j \pm 2$ population transitions [8]. The terahertz coupling term $T_{j,k}^m = \langle j,m|\cos(\theta)|k,m\rangle$ is zero unless $j = k \pm 1$, so terahertz radiation drives coherence between states of opposite parity, and is resonantly absorbed and emitted by $j \to j \pm 1$ transitions at frequency $\omega_{j,j+1}$. Finally, $(d\rho_{j,k}^m/dt)_{\text{diss}}$ accounts for dissipative effects like collisions which drive the gas towards thermal equilibrium [5].

In thermal equilibrium at temperature T, the population of rotational states $\rho_{j,j}^m$ is given by Boltzmann statistics:

$$\frac{\rho_{j,j}^m}{\rho_{0,0}^0} = \exp\left(\frac{-\hbar\omega_j}{k_B T}\right) \qquad (2)$$

Where k_B is Boltzmann's constant. In thermal equilibrium there is no coherence between molecules and no preferred direction, so $\rho_{j,k\neq j}^m = 0$ and we normalize $\boldsymbol{\rho}$ such that $\sum_{j,m}\rho_{j,j}^m = 1$. Our simulations apply a sequence of optical and terahertz pulses to an intially thermal HCN gas, and the resulting changes in population $\Delta\rho_{j,j}^m$ give the average energy absorbed/emitted per molecule $\Delta E = \sum_{j,m}\hbar\omega_j\Delta\rho_{j,j}^m$ from each of the pulses. Since we neglect back-action of the molecular emission on the ensemble, we can calculate transitions driven by the applied pulses but not self-stimulated transitions like those observed in free-induction decay [3].

3. Amplification

As shown in Fig. 2, a series of short intense optical pulses can drive HCN gas into an excited, inverted rotational state suitable for broadband terahertz amplification. Figure 2(a) shows the initial rotational population of the gas in thermal equilibrium at 310K: $\rho_{j,j}^m$ decreases with j and is independent of m. Illumination by a single 15TW/cm^2, 100fs, 800nm optical pulse drives coherence ($|\rho_{j,k\neq j}^m| > 0$) between the gas molecules, but as shown in Fig. 2(b), causes little change in the rotational populations $\rho_{j,j}^m$. Arbitrarily increasing the intensity of the optical
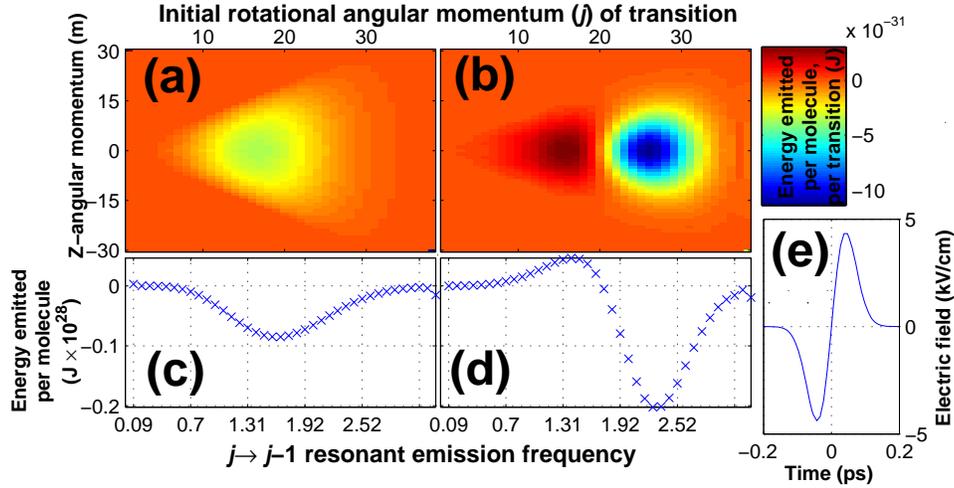
Fig. 3. Energy absorbed/emitted by 200fs-pulse THz-driven $j \to j \pm 1$ transitions vs. j and m of the upper state for (a) an initially thermal HCN gas and (b) the optically-excited rotational populations shown in Fig. 2(c, f). Summed over m, this gives energy absorbed/emitted near each resonant frequency $2jf_0$ for c thermal and d excited gas. The ~ 200fs terahertz pulse driving these transitions (e) follows at $T_r/2$ after the last optical excitation pulse.

pulse would drive larger changes in the rotational populations, but would also cause undesired effects like vibrational excitation, self-focusing, or ionization.

Luckily, a *train* of pulses can drive *much* larger changes in rotational populations. At low gas pressures ($\ll 1$ atm) collisions are rare and $(d\rho_{j,k}^m/dt)_{\text{diss}} \ll f_0^{-1}$. The field-free $\boldsymbol{\rho}(t)$ of a rigid-rotor gas is then perfectly periodic with period $T_r = (2f_0)^{-1}$, and a sequence of small pulses separated by T_r build up resonantly to the same effect as one big pulse with the same total energy. In Fig. 2(c), four 15TW/cm^2, 100fs, 800nm optical pulses separated by $T_{r,HCN} = 11.49$ps strongly invert the population of the HCN gas; each molecule absorbs $\sim 4.6 \times 10^{-21}$J of rotational energy. $\rho_{j,j}^m$ increases with j for nearly every transition from $j = 5$ to $j = 19$; a broadband terahertz pulse could be amplified simultaneously by all these transitions. The optical pulses drive population to higher j values by strongly aligning the molecules; a rigid rotor highly localized in θ must occupy broad spectrum of j states, and tighter angular localization projects into higher j.

The simulation results are identical (neglecting ionization) to a single pulse with intensity 60TW/cm^2. Impressively, a train of 600, 0.1TW/cm^2 pulses separated by T_r gives the same result. Splitting the pulse energy into a train of smaller pulses avoids undesired intensity-dependent effects, and would allow recycling the same optical pulse in a cavity for high efficiency. The number of times a pulse can be reused for pumping is limited by the pressure-dependent alignment lifetime; the results in Fig 2(c, f) are appropriate for pressures $< 10^{-2}$ atmospheres.

Figure 3 shows the effect of this four-pulse optical excitation on HCN's terahertz absorption. At 310K without excitation, the $j \to j - 1$ spectral lines are purely absorptive (Fig. 3(a, c)) at resonant frequencies $2jf_0$ when illuminated with the broadband single-cycle pulse shown in Fig 3(e). The width of these absorption lines depends on pressure; the HCN $j = 0 \to 1$ linewidth $2\Delta f \approx 38$GHz/atm [9], corresponding to an alignment lifetime of ~ 200ps at 0.02 atm pressure.

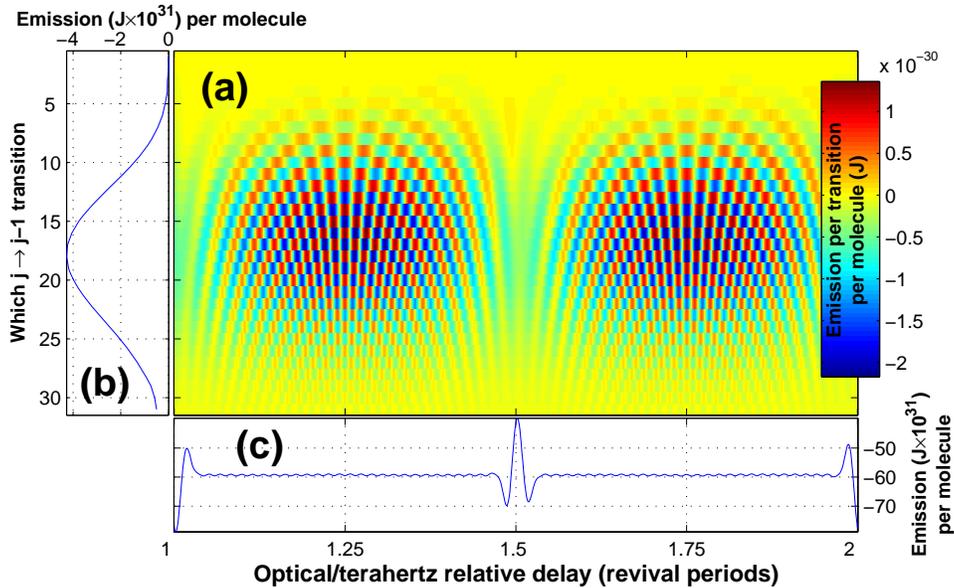However, if the same terahertz pulse follows $T_r/2$ behind the last optical excitation pulse

Fig. 4. Energy absorbed/emitted by 800fs-pulse terahertz-driven $j \rightarrow j \pm 1$ transitions vs. j and m of the upper state for (a) an initially thermal HCN gas and (b) the optically-excited rotational populations shown in Fig. 2(c, f). Summed over m, this gives energy absorbed/emitted near each resonant frequency $2jf_0$ for c thermal and d excited gas. The ~ 800fs terahertz pulse driving these transitions the 19 lowest absorptionthe 19 lowest absorption(e) follows at $T_r/2$ after the last optical excitation pulse.

from Fig. 2(c), the 19 lowest absorption lines become amplification lines. This comb of amplification frequencies extends from 0.08 THz to 1.6 THz, as shown in Fig. 3(b, d) and the degree of amplification is comparable to the degree of absorption without excitation. In the 0-1.6 THz band, each unexcited HCN molecule would absorb about $\sim 6.4 \times 10^{-29}$J of energy; with excitation, each molecule instead emits $\sim 3.6 \times 10^{-29}$J. The seed terahertz pulse has a fluence of about 5nJ/cm^2, which could be generated in femtosecond-illuminated ZnTe. Extracting 3.6×10^{-29}J from each molecule means a small-signal gain of about 0.85nJ/cm^2 per centimeter of propagation, per atmosphere of HCN pressure. After propagating only a few centimeters, the high-frequency component (> 1.6THz) of the seed pulse's spectrum will be completely absorbed and the remaining amplified spectrum will closely match the amplification band ($0 - 1.6$THz), indicating significant pulse reshaping.

The ~ 200fs terahertz pulse used in Fig. 3 is too short to be efficiently amplified, since most of its spectrum lies above the 0-1.6 THz amplification band. Figure 4 shows the same calculation for a longer (~ 800fs) terahertz pulse with the same fluence. The longer pulse better overlaps both the amplification and thermal absorption bands. In the 0-1.6 THz band, each unexcited HCN molecule would absorb about $\sim 8 \times 10^{-28}$J of energy; with excitation, each molecule instead emits $\sim 3 \times 10^{-28}$J, giving a more respectable gain of 7.1nJ/cm^2 per centimeter of propagation per atmosphere of HCN. Note also that there is very little absorption of this pulse by the excited molecules shown in Fig. 4(b, d), indicating little pulse reshaping.

This extracted energy is less than 10^{-6} of the absorbed optical pump energy. Maximum extractable energy can be estimated because the first three optical pump pulses drive HCN to the cusp of inversion, and only the fourth optical pump pulse drives population inversion. A strong terahertz pulse which saturates extraction would drive the populations back to this uninverted state, extracting 41mJ/cm^3 per atmosphere of pressure. Saturated extraction will generally drive population transitions and nonlinear effects, but the 5nJ/cm^2 terahertz pulse fluence studied here is well below saturation; doubling the terahertz intensity (not shown) pre-

Fig. 5. A 1TW/cm^2 optical pulse weakly aligns HCN and strongly modulates **(a)** terahertz energy absorbed/emitted per molecule, per $m = 0$, $j \rightarrow j - 1$ transition depending on the optical-terahertz relative delay ΔT. (b) Averaging over delay shows the 'incoherent' absorption that a terahertz pulse would experience if it was not collinear with the optical pump pulses. (c) Summing over j gives total absorption vs. ΔT.

cisely doubles the extracted energy from each transition. Extraction of less than 100 $\mu J / \text{cm}^3$ per atmosphere would leave the rotational populations changed by less than one part in 500.

The temporal shape of this emission depends on collisions. The time-domain simulation used here only calculates the energy ΔE absorbed or emitted while the seed pulse interacts with the molecules, so post-pulse terahertz emission is not considered. At low pressures ($\ll$ 1atm), in addition to absorbing or amplifying the original pulse, molecular rotations will remain coherent for many T_r and will also generate a following train of few-cycle terahertz pulses spaced by T_r [3]; this is beyond the scope of our simulation. However, use of a cavity to pass the terahertz pulse repeatedly through the excited low-pressure gas allows collection of this excess energy into the original seed pulse, further increasing gain.

4. Coherent Effects

The terahertz amplification shown in Figs. 3 and 4 is for a terahertz pulse copropagating with the optical excitation pulses with constant relative delay $\Delta T = T_r/2$. Interestingly, varying the relative delay between the optical and terahertz pulses can strongly modulate the terahertz absorption or amplification, as shown in Fig. 5. A 1TW/cm^2, 100fs optical pulse weakly aligns the HCN molecules ($|\rho_{j,k \neq j}^m| > 0$ with common phase at $t = 0$) while driving negligible change in populations ($\rho_{j,j}^m \approx \rho_{j,j,\text{thermal}}^m$). The same $\sim$ 200fs input terahertz pulse as Fig. 3 follows the optical alignment pulse with variable ΔT; HCN's rotational absorption/emission is wildly modulated by this alignment depending on ΔT. For clarity and computational reasons we show only the $m = 0$ case, but the behavior is similar for all m.

A terahertz pulse copropagating with the optical excitation pulse would have roughly constant ΔT, and absorption could be enhanced ($\Delta T = nT_r$, where n is an integer), suppressed (
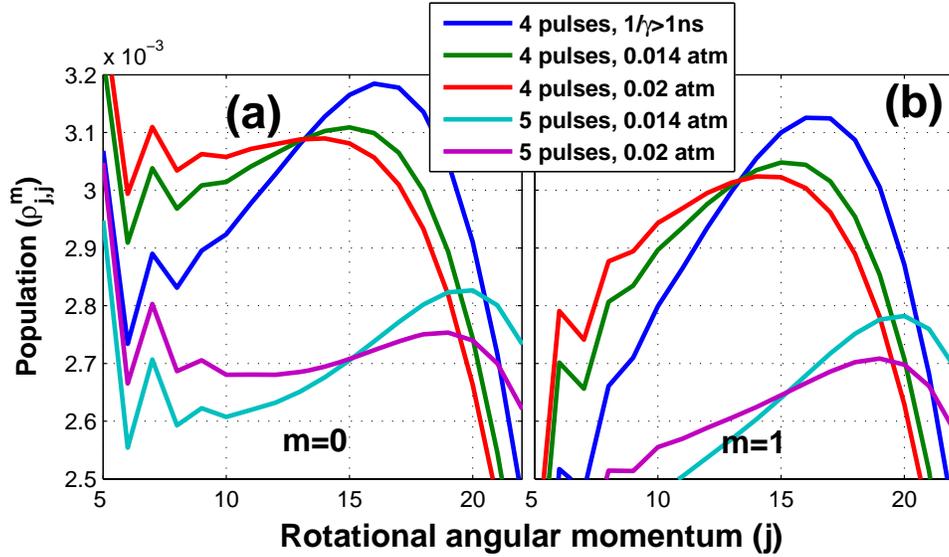
Fig. 6. Population $\rho_{j,j}^{m}$ for different dissipation rates γ and number of optical pump pulses for (a) $m = 0$ and (b) $m = 1$.

$\Delta T = (n + 1/2)T_r$), or oscillatory in spectrum, as shown in Fig. 5(a, c). If the terahertz pulse is propagating at some angle to the optical beam path, then ΔT will slip, and the terahertz absorption will average over delays as shown in Fig. 5(b). This 'incoherent' absorption depends mainly on populations $\rho_{j,j}^{m}$ rather than coherences $\rho_{j,k \neq j}^{m}$, as in [3].

5. Pressure and temperature effects

High pressures are desirable for high single-pass gain and high saturation energy. Low pressures are desirable because they allow many optical pulses to contribute to the population inversion; a compromise is necessary. In general, the dissipation of the density matrix toward thermal equilibrium is complicated [5] and not well studied experimentally, so we adopt the simple model $(d\rho_{j,k}^{m}/dt)_{\text{diss}} = \gamma(\rho_{j,k}^{m} - \rho_{j,k,\text{thermal}}^{m})$. As shown in Fig. 6, for very low pressures ($1/\gamma > 1$ns), four-pulse optical pumping drives a strong population inversion, but dissipation in the range $1/\gamma = 200 - 300$ps (corresponding to pressures of ~ 0.01 atm) decreases the strength and the bandwidth of the population inversion for the $m = 0,1$ cases (other m's are similar). Increasing the number of pump pulses from four to five, however, returns some of the inversion strength and more than restores the bandwidth. Estimating $\Delta\nu_{j-1,j} \approx \Delta\nu_{0,1}$ and $\gamma \approx 2\pi\Delta f$, these decay times are appropriate for a pressure of ~ 0.014 ($1/\gamma = 300$ps) and 0.02 ($1/\gamma = 200$ps) atmospheres [9].

Gain at these pressures would be fairly low. Decreasing temperature to decrease collisions without sacrificing density is appealing, but HCN's vapor pressure drops off rapidly for temperatures below 300K. The use of a gas jet rather than a static gas target allows the use of higher density targets at lower rotational temperature and long collision times [10]. As shown in Fig. 7, a low temperature ($T = 50$K) HCN gas jet target gives a much stronger population inversion after four-pulse optical pumping than in uncooled ($T = 310$K) static HCN, resulting in much more gain per molecule. Additionally, low temperatures concentrate population in low m-states which have a larger effective dipole interaction with terahertz fields. Estimating $\gamma_{\text{jet}} = \gamma_{\text{static}}\sqrt{T_{\text{jet}}/T_{\text{static}}}$ at comparable density, collisional decay would be 2.5 times slower in a
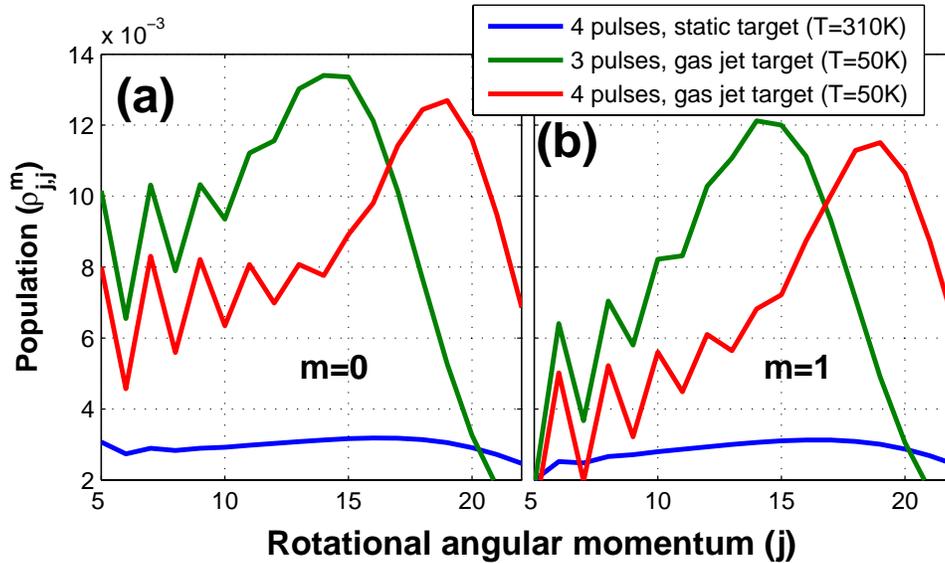
Fig. 7. Population $\rho_{j,j}^m$ for static gas and gas jet initial temperatures T for **(a)** $m = 0$ and **(b)** $m = 1$, neglecting collisions ($1/\gamma \gg 1$ns).

gas jet. The lower temperature of the gas jet also makes population inversion easier to achieve. At low pressures ($1/\gamma \gg 1$ns), only three optical pulses still drive a strong population in 50K HCN, although with a reduced inversion bandwidth.

6. Conclusion

Unlike conventional CW terahertz lasers [11], this wide band of regularly-spaced rotational lines can amplify a short, possibly single-cycle broadband terahertz pulse. Unlike rotational lasers driven by pumping single vibrational transitions with CO_2 lasers [12], several tens of rotational lines are simultaneously driven to population inversion which can simultaneously amplify a single pulse, allowing a lasing bandwidth of hundreds of GHz. Unlike coherent terahertz generation methods such as optical rectification or photoconductive antennae which must be scaled to large apertures to achieve high pulse energies, this amplification medium can be multi-passed to reach high terahertz energies. The molecules simulated in Fig. 2 absorb nearly 30 milli-eV of rotational energy per molecule, so energy extraction could saturate at hundreds of $\mu J/\text{cm}^3$ or more. Since this method is not sensitive to the temporal shape of the optical pump pulse, the same pump pulse could be recycled in a cavity or multipass configuration to achieve high coupling efficiency. Rotational lasing in aligned molecules could open the field of very high field terahertz optics to small laboratories.